# Computer Simulation Studies of PEO/Layer Silicate Nanocomposites

E. Hackett, E. Manias,* and E. P. Giannelis†

*Department of Materials Science and Engineering, Cornell University, Ithaca, New York 14853*

*Received October 22, 1999. Revised Manuscript Received April 4, 2000*

Monte Carlo and molecular dynamics computer simulations are used to explore the atomic scale structure and dynamics of intercalated PEO/montmorillonite nanocomposites. Particular attention is paid to the configuration of the polymer within these confined spaces. A layered, but disordered and liquid-like, structure is observed, in contrast to the all-trans or helical extended interlayer structures traditionally suggested. The cations primarily reside near the silicate surface. Molecular dynamics simulations also provide information on the interlayer mobility of $Li^+$ ions, which is related to the ionic conductivity in polymer electrolyte nanocomposites.

## I. Introduction

Nanocomposites composed of poly(ethylene oxide) (PEO) intercalated between the layers of mica-type silicates represent a new class of polymer composite electrolytes.[1−9] They possess novel mechanical and electrical properties that render them very promising materials for applications such as solid-state lithium batteries. A better understanding of the structure and dynamics of the intercalated polymers in these nanocomposites can provide molecular insight and lead to the design of materials with improved properties.

Mica-type layer silicates share the same structural characteristics as the better known talc and mica. Their crystal lattice consists of negatively charged aluminosilicate layers. These layers are negatively charged, and in their pristine form this charge is balanced by hydrated cations ($Li^+$, $Na^+$, or $Ca^{2+}$) that occupy the spaces between the layers (galleries). PEO can be intercalated, or inserted, between these layers by replacing, partly or completely, the water molecules occupying the interlayer. This can be accomplished by melt intercalation, in which a dry PEO/silicate mixture is heated above the melting temperature ($T_m$) of the PEO, at which point it spontaneously intercalates as observed by X-ray diffraction.[5] Alternatively, the nanocomposite can also be prepared from an aqueous solution,[4,6] resulting in nanocomposite structures similar to those prepared by the melt intercalation method. In the nanocomposites, PEO forms the matrix for a solid state electrolyte whose conductivity is primarily cationic because the anions are the large silicate layers. Furthermore, the intercalated polymers of the nanocomposite do not exhibit any marked melting transition near the bulk $T_m$ of PEO, and at temperatures below $T_m$, they promote much higher cationic conductivities than the respective bulk PEO/alkali systems. In addition, the polymer chains in the nanocomposite show significant mobility, even at temperatures well below the bulk $T_m$.[5]

The polymer chains and silicate layers self-assemble in an alternating fashion with a periodic *d* spacing of 18 ± 1 Å, of which 9.7 Å corresponds to the silicate layer.[4,6] The polymer chains are confined within 8 ± 1 Å, only a few atomic diameters wide. This extreme confinement has a profound effect on the structure of the intercalated polymer. Additionally, the interactions between the alkali cations, the negatively charged silicate layers, and the polymer are important in understanding the structure of the nanocomposite as well as its conductivity. In addition, recent work[6] has shown that a small amount of water is present in the nanocomposite galleries when PEO is intercalated from solution. The computer simulations presented here study first the structure at the atomic level of intercalated PEO nanocomposites. Molecular dynamics simulations provide insight into the mobility of $Li^+$ ions and the role that the cations' hydration shells plays in the cation conductivity. Dry and hydrated nanocomposites were studied and the effects of hydration on the structure and cation mobility are discussed.

## II. Model

All simulations were performed using Cerius[2] software, although most of the data analysis utilized programs developed especially for this nanocomposite system. The force fields used in this simulation study are based on a geometrically fitted and optimized

* Current address: Department of Materials Science and Engineering, The Pennsylvania State University, 310 Steidle Bldg., University Park, PA 16802. E-mails: eh42@msc.cornell.edu; manias@psu.edu; epg2@cornell.edu.

(1) Aranda, P.; Ruiz-Hitzky, E. *Chem. Mater.* **1992**, *4*, 1395−1403.
(2) Ruiz-Hitzky, E.; Aranda, P. *Adv. Mater.* **1990**, *2*, 545.
(3) Aranda, P.; Galvan, J. C.; Casal, B.; Ruiz-Hitzky, E. *Electrochim. Acta* **1992**, *37*, 1573.
(4) Wu, J.; Lerner, M. M. *Chem. Mater.* **1993**, 5, 835−838.
(5) Wong, S.; Vaia, R. A.; Giannelis, E. P.; Zax, D. B. *Solid State Ionics* **1996**, 86, 547−57.
(6) Bujdak, J.; Hackett, E.; Giannelis, E. P. *Chem. Mater.* **2000**, *8*, 2168.
(7) Vaia, R. A.; Vasudevan, S.; Krawiec, W.; Scanlon, L. G.; Giannelis, E. P. *Adv. Mater.* **1995**, *7*, 154.
(8) Vaia, R. A.; Sauer, B. B.; Tse, O. K.; Giannelis, E. P. *J. Polym. Sci. Polym. Phys.* **1997**, *35*, 59.
(9) Hutchison, J. C.; Bissesseur, R.; Shriver, D. F. *Chem. Mater.* **1996**, *8*, 1597−1599.

10.1021/cm990676x CCC: $19.00 
Published on Web 07/07/2000

combination of force fields used in previous studies of hydrated montmorillonite[10−12] and PEO−salt systems.[13,14] Silicate atoms have been completely constrained in all cases. Monte Carlo absorption simulations were carried out using an MCY water model with an offset oxygen charge, while for molecular dynamics (MD) simulations a modified MCY model in which the charge was centered at the atom centers produced adequate results.

The cation exchange capacity (CEC), which is a characteristic of the silicate and provides the charge on the silicate layers, determines the number of compensating cations in the gallery. The CEC of the silicates studied here is set to ≈105 mequiv/100 g. This is a common CEC for montmorillonite,[31] and corresponds to the silicate studied in the experimental counterpart to this work.[6] The simulation box uses periodic boundary conditions and is 42.24 × 36.56 Å in the direction parallel to the silicate, while the third dimension is determined by the periodic repeat distance, or *d* spacing, which is measured by X-ray diffraction.

A *d* spacing of 18 Å was used for the $Li^+$ −montmorillonite/PEO nanocomposite. After MD simulations of up to 50 000 time steps (0.1 ns) of the dry $Li^+$−montmorillonite/PEO system, which served to equilibrate the polymer configuration and provide structural information for the dry system, water was adsorbed through a grand canonical Monte Carlo (GCMC) simulation in which chemical equilibrium was established by imposing a water vapor pressure of 100 kPa (1 atm). The hydrated system was equilibrated with further MD simulation in an NVT ensemble. The water molecules were subsequently deleted and readsorbed through a second GCMC run that ensured an accurate amount of adsorbed water. The amount of water from these simulations is in very good agreement with the amount of water measured experimentally,[6] providing a useful check on the validity of the force field used here. After the water was adsorbed, several NVT MD simulations of up to 500 000 time steps (1 ns), at a temperature of 300 K, were carried out from various initial system configurations. Configurations were saved every 500 steps, and the stored trajectories were used to calculate the equilibrium structure and dynamic information presented here.

In the case of $Na^+$−montmorillonite, a *d* spacing of 17.6 Å was used. Several productive simulation runs, typically of 50 000 time steps (0.1 ns), were carried out from various initial configurations.

## III. Results and Discussion

A snapshot of the hydrated Li−montmorillonite system is shown in Figure 1. Although this is a snapshot of a particular water-containing system, it illustrates many of the features, discussed in detail below, that are apparent in both dry and hydrated systems. These features include the preferred locations of ions and the disordered bilayer structure of the polymer.

Number density profiles showing the arrangement of $Li^+$ or $Na^+$ and polymer in the silicate gallery of the dry systems through a plane normal to the silicate surfaces are shown in Figure 2. Both the oxygen and carbon density profiles as well as the profiles of the polymer as a whole indicate a bilayer structure, with the thickness of each layer approximately equal to a PEO chain width as calculated from the known molecular structure. Such layer structures originate from the oscillating solvation forces near a surface. Their existence is suggested by several experimental and computer studies of nanoscopically confined fluids and polymers[15−28] including previous experimental observations of PEO intercalated in layer silicates that imply the existence of one or two intercalated layers.[1−9] In this layer structure confined chain molecules tend to align themselves parallel to the wall so that large segments of a chain will lie within a single layer, which is seen as a peak in the density profile (Figure 2). At the same time, the polymer chains are relatively disordered in the plane parallel to the silicate surface. Chains may twist around each other or span across the polymer layers within the gallery. Despite the layered ordering normal to the surfaces, the polymer configurations exhibit a disordered, almost liquid-like, structure. These findings contrast previous suggestions in which an all-trans extended bilayer or a helical structure for the polymer was proposed.[1]

The cations for both dry systems are bound to the wall (Figure 2), about 1.5 Å from the center of the surface oxygen atoms, or about 4.8 Å from the central plane of metal atoms, in very good agreement with NMR data.[29] Surface lattice cavities are characteristic of the oxygen network in all 2:1 layer silicates, and the cations primarily reside partially inserted within these cavities. Although the $Li^+$ ions are smaller than the $Na^+$ ions and their density profiles extend into the surface cavities, the $Li^+$ density profiles have their largest peaks slightly outside these cavities (Figure 2). The cations' locations, as revealed by the simulations, contrast with the assumption that the cations are located in the middle of the gallery.[1] In addition, this agrees with the location of cations as shown in NMR data.[29] The location

(10) Chang, F. C.; Skipper, N. T.; Sposito, G. *Langmuir* **1997**, *13*, 2074−2082.
(11) Skipper, N. T.; Chang, F. C.; Sposito, G. *Clays Clay Miner.* **1995**, *43*, 285−293.
(12) Manias, E.; Chan, Y. K.; Giannelis, E. P.; Panagiotopoulos, A. Z.; Zax, D. B. CMS Workshop Lectures, The Clay Minerals Society, in press.
(13) Muller-Plathe, F. *Acta Polym.* **1994**, *45*, 259−293.
(14) Smith, G. D.; Jaffe, R. L.; Yoon, D. Y. *J. Phys. Chem.* **1993**, *97*, 12752−12759.
(15) Horn, R. G.; Israelachvili, J. N. *J. Chem. Phys.* **1981**, *75*, 1400.
(16) Christenson, H. K. *J. Chem. Phys.* 1983, *78*, 6906.
(17) Chan, D. Y. C.; Horn, R. G. *J. Chem. Phys.* **1985**, *83*, 5311.
(18) Israelachvili, J. N.; Kott, S. J. *J. Chem. Phys.* **1988**, *88*, 7162.
(19) Montfort, J. P.; Hadziioannou, G. *J. Chem. Phys.* **1988**, *88*, 7187−96.
(20) Gee, M. L.; McGuiggan, P. M.; Israelachvili, J. N.; Homola, A. M. *J. Chem. Phys.* **1990**, *93*, 1895−906.
(21) Israelachvili, J. *Intermolecular and Surface Forces*, 2nd ed.; Harcourt, Brace, Jovanovich: New York, 1992.
(22) Ribarsky, M. W.; Landman, U. *J. Chem. Phys.* **1992**, *97*, 1937.
(23) Xia, T. K.; Ouyang, J.; Ribarsky, M. W.; Landman, U. *Phys. Rev. Lett.* **1992**, *69*, 1967.
(24) Bitsanis, I. A.; Pan, C. *J. Chem. Phys.* **1993**, *99*, 5520.
(25) Gupta, S.; Koopman, D. C.; Westermann-Clark, G. B.; Bitsanis, I. A. *J. Chem. Phys.* **1994**, *100*, 8444.
(26) Padilla, P.; Toxvaerd, S. *J. Chem. Phys.* **1994**, *101*, 1490.
(27) Manias, E.; Hadziioannou, G.; ten Brinke, G. *Langmuir* **1996**, *12*, 4587.
(28) Hackett, E.; Manias, E.; Giannelis, E. P. *J. Chem. Phys.* **1998**, *108*, 7410.
(29) Yang, D.-K.; Zax, D. B. *J. Chem. Phys.* **1999**, *110*, 5325.

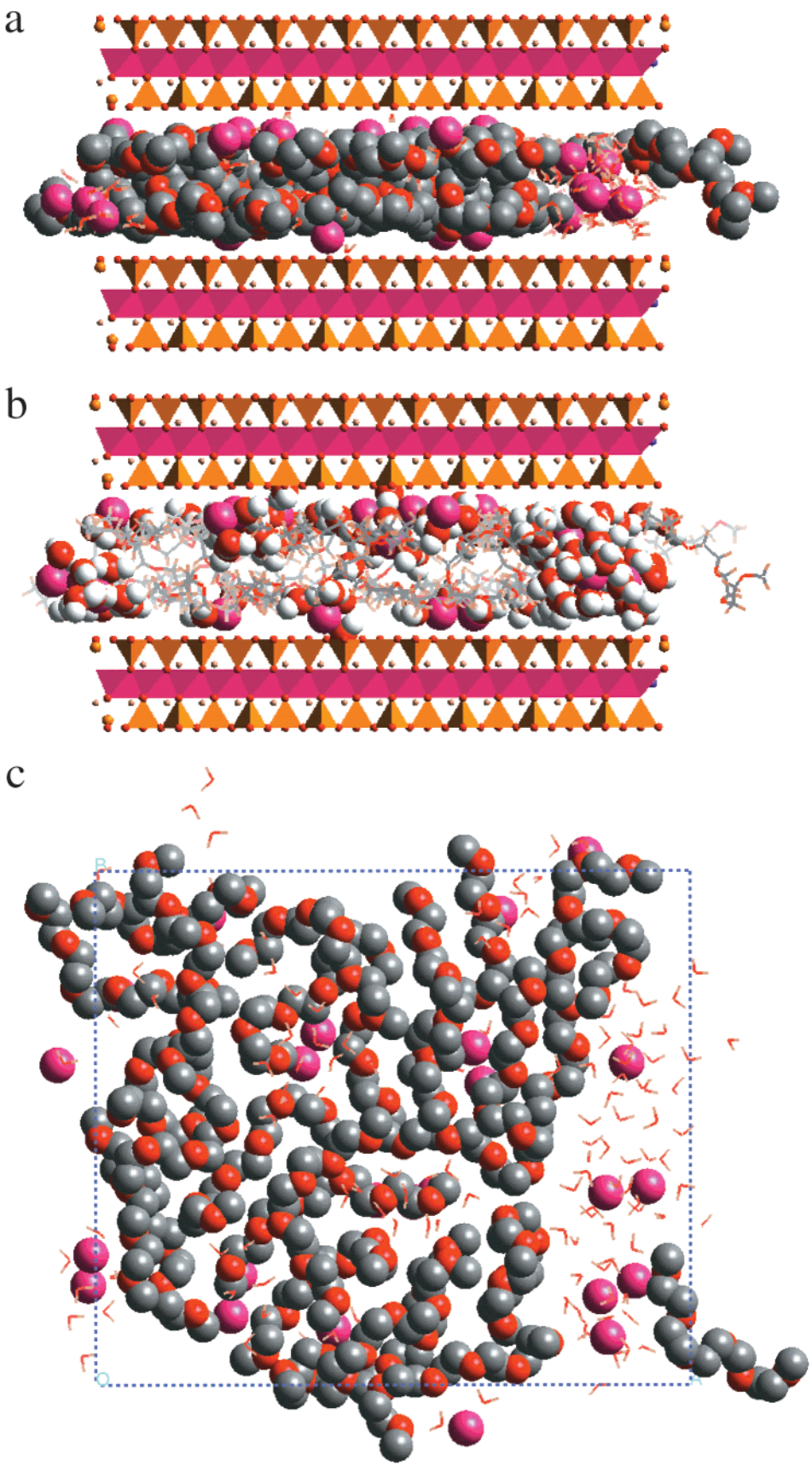


**Figure 1.** Snapshot of PEO−silicate nanocomposite: (a) showing the silicate crystal as polyhedra, $Li^+$ as spheres, and highlighting PEO as spheres; (b) showing the silicate crystal as polyhedra, $Li^+$ as spheres, and highlighting water as spheres; (c) top view with silicate removed, showing PEO and $Li^+$ as spheres and water as sticks.

of the cations in the interlayer gallery becomes very important for these materials because, as will be discussed below, it affects the cationic mobility.

Density profiles for the hydrated PEO/$Li^+$−montmorillonite system are shown in Figure 3, corresponding to the snapshot of the system shown in Figure 1. The

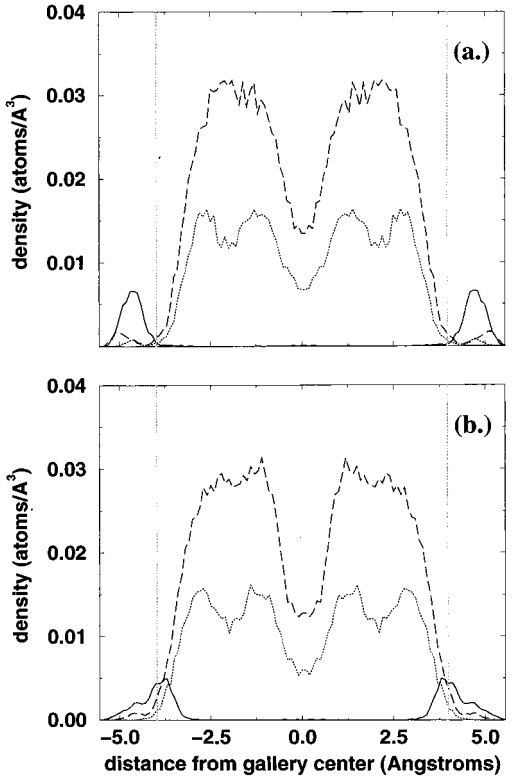


**Figure 2.** Density profiles normal to the silicate layers for (a) $Na^+$−montmorillonite and (b) $Li^+$−montmorillonite PEO nanocomposites. Solid line, cation ($Na^+$ or Li); dotted line, PEO oxygen; dashed line, PEO carbon. Left and right graph boundaries correspond to the plane containing the centers of the surface oxygen atoms; pale gray vertical lines represent the outer edge of the surface oxygen layer. The pale gray dotted horizontal line represents the average atomic carbon density of bulk PEO as calculated from a handbook density for the bulk polymer (1.1 g/cm$^3$).

bilayer structure of the polymer in this system is even more pronounced, and the disordered nature of the chain configurations can be seen clearly from the snapshot (Figure 1). Again, the liquid-like structure contrasts with previous suggestions of helical or all-trans extended polymer structures within the gallery.[1]

The observed configurations are also in very good agreement with small-angle neutron scattering (SANS) experiments. SANS profiles from 15 K to room temperature can only be simulated by assuming a disordered polymer configuration.[30] Integration of the density profiles (Figure 3) shows that slightly more than half of the ions reside in layers very near the silicate surface (<2.5 Å from the surfaces).

The density profile of Li inside the interlayer gallery of the hydrated system is quite different than that of the dry Na or Li systems. As before, some Li ions are located <2 Å from the surface, partially inserted within the surface lattice cavities, but now there also exists a large number of Li ions inside the galleries. They form two diffuse layers as the density profiles show (Figure 3).

In the long simulation of the hydrated system, few atoms were exchanged between the surface layers and gallery center over the time scale of this simulation (1

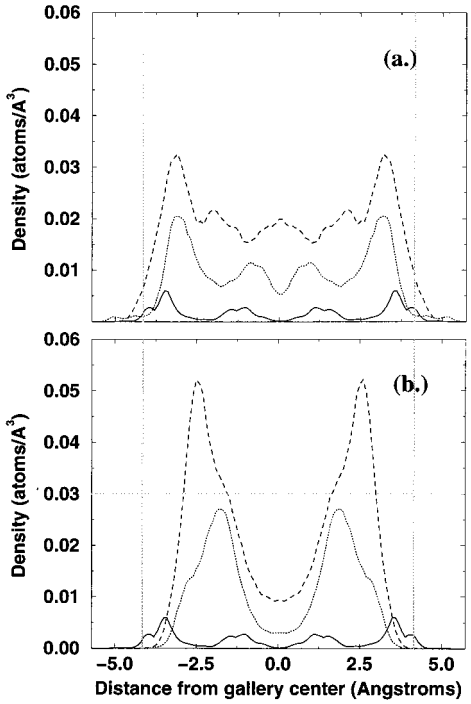


**Figure 3.** Density profiles within the silicate gallery for the hydrated $Li^+$−montmorillonite/PEO nanocomposite: (a) Solid line, $Li^+$; dotted line, water oxygen; dashed line, water hydrogen. (b) For the same systems as those in (a): solid line, $Li^+$; dotted line, PEO oxygen; dashed line, PEO carbon. Left and right graph boundaries correspond to the plane containing the centers of the surface oxygen atoms; pale gray lines represent the outer edge of the surface oxygen layer.

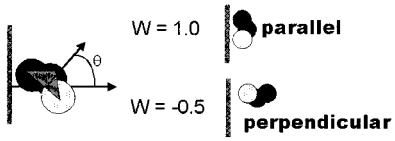


**Figure 4.** Schematic diagram of an idealized C−C−O bond and the silicate surface illustrating the definition of $\theta$ used in the calculation of the order parameter and the bond configurations corresponding to the upper and lower limits of possible values for the order parameter.

ns). The small, outer shoulder of this first density peak is due to ions that have dropped into the crystalline cavities of the silicate surface. The water density profiles have a similar shape to the $Li^+$ density profiles, with the exception of this outer shoulder, suggesting that the water predominantly exists in hydration shells around the $Li^+$ ions, as can be directly observed from the system configurations through radial pair correlation functions (PCF), which are discussed below. In contrast, PEO density maxima occur between the minima where the $Li^+$ and water densities are relatively low, almost in the same positions as those in the dry systems but characterized here by narrower layer widths.

An order parameter can be defined that describes the orientation of the PEO bond angles.[22−27] If $\theta$ is the angle between the normal to the plane formed by a C−C−O bond and a normal to the silicate surface, as illustrated schematically in Figure 4, an order parameter, $W$, can be defined as

$$W = \frac{1}{2}\langle 3\cos^2\theta - 1\rangle \qquad (1)$$

(30) Krishnamoorti, R. K.; Giannelis, E. P. unpublished data.
(31) Solomon, D. H.; Hawthorne, D. G. *Chemistry of Pigments and Fillers*; Kreiger Publishing Co.:Malabar, FL, 1991.

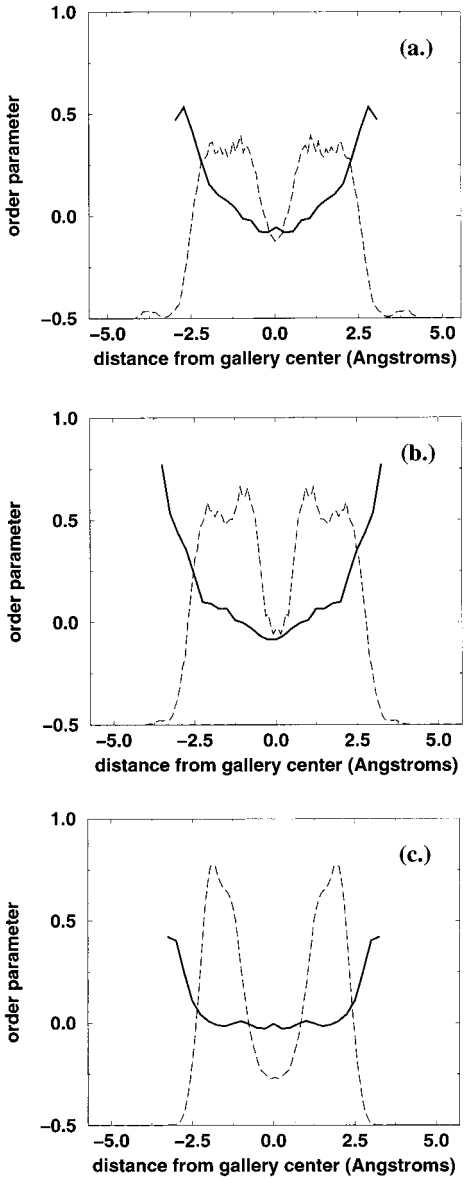


**Figure 5.** Order parameter of C−C−O bonds (solid lines) as a function of position in the silicate gallery. An order parameter of one implies that bonds lie flat against the surface, while random bond angle orientation results in an order parameter of approximately zero. The PEO (carbon and oxygen) density profiles (dashed lines) are shown for comparison. (a) Dry $Na^+$−montmorillonite/PEO nanocomposite; (b) dry $Li^+$−montmorillonite/PEO nanocomposite; (c) hydrated $Li^+$−montmorillonite/PEO nanocomposite.

For $\theta = 0°$, corresponding to C−C−O bonds on planes flat against the surface, the order parameter will be equal to 1. For $\theta = 90°$, meaning that a C−C−O bond lies normal to the surface, the order parameter is −0.5. These limiting cases are illustrated in Figure 4. An order parameter of approximately zero indicates random bond orientation.

Figure 5 shows the order parameter as a function of the bond position inside the gallery for the nanocomposites studied here. The bonds with a center of mass nearest the silicate surface have an order parameter of 0.5 or higher, indicating that these bonds are inclined to lie flat against the surface. Such surface-induced, or epitaxial, orientations next to the confining wall is expected. In the dry systems, which have more atomic-level ordering, as seen in the finer details of their oxygen and carbon density profiles compared to those of the hydrated system, this ordering of the bonds extends a few Angstroms—less than a single atomic layer—further into the gallery. However, for the hydrated systems, this bond orientation does not extend any significant distance into the gallery. The bonds that are not directly on the silicate surface do not show any preferred orientation. The calculated average order parameter of C−C−O bonds for the whole PEO intercalated film is 0.06 for the dry and 0.03 for the hydrated $Li^+$−montmorillonite, respectively, showing a nearly random distribution of C−C−O bonds with respect to the silicate surface in both cases. It is likely that the bonds are unable to maintain a vertical orientation, as the spacing may suggest, because of the frequent obstacles caused by cations and water molecules. Also, the layer distribution of oxygen, as indicated by the density profiles, cannot be achieved with a strictly horizontal or vertical bond angle orientation of the ethylene oxide repeat unit. The additional layering, and to a lesser extent, ordering, of the oxygen in the dry $Na^+$ or $Li^+$/PEO intercalated system is most likely due to the oxygen's effort to coordinate to the cations, rather than the confinement-induced ordering of the chain conformations. This feature disappears with the introduction of water, which replaces PEO oxygen in the cation coordination shells. In the water-containing systems, the polymer coordinates less to the cation, and thus it can more freely organize into a more pronounced bilayer, which is the configuration dictated by the steric constraint.

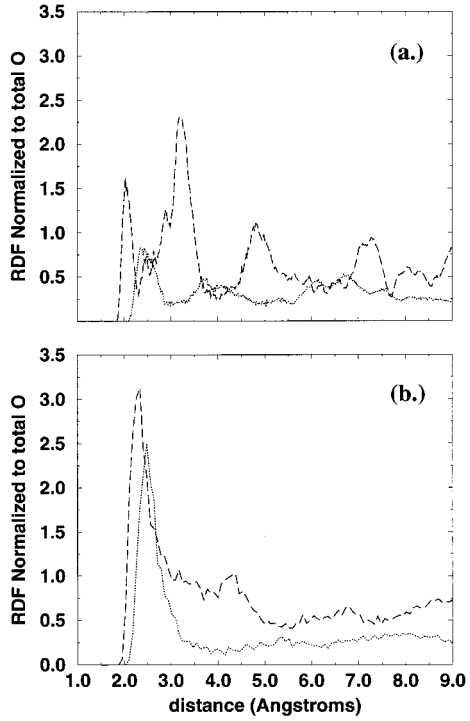


**Figure 6.** Radial pair correlation functions of cations and oxygen for the dry PEO nanocomposites: (a) Na−montmorillonite; (b) Li−montmorillonite. For both graphs: dashed line, PCF with silicate surface oxygens; dotted line, PCF with PEO oxygens.

Radial pair correlation functions (PCF), shown in Figures 6 and 7, illustrate the degree of association between the cations and the various species containing oxygen in the system. The area under the first peak in

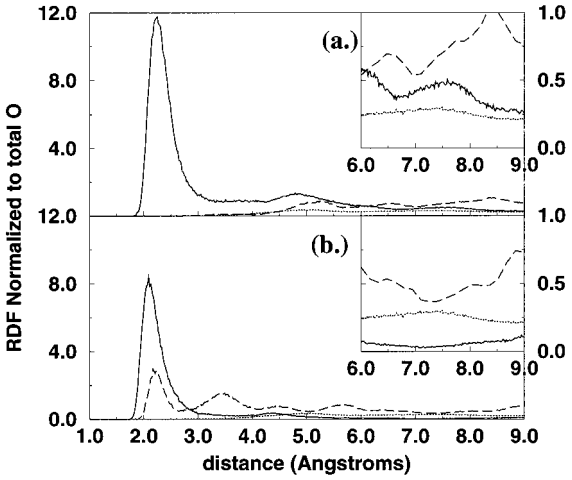


**Figure 7.** Pair correlation functions of $Li^+$ ions and oxygen for the hydrated $Li^+$−montmorillonite/PEO nanocomposites. Insets show convergence at long distances. (a) Gallery center $Li^+$; (b) silicate surface $Li^+$. Solid line, PCF with water oxygen atoms; heavy dashed line, PCF with silicate surface oxygens; light dotted line of both graphs, PCF between all $Li^+$ and PEO oxygens.

the PCF represents the coordination between the cation and the type of oxygen being considered. In this two-dimensional system, PCFs cannot be assumed to provide the accurate topological information about the cations' coordination. However, whereas the density profiles average the structure throughout a given plane parallel to the silicate, the PCFs provide information pertinent to the ions' immediate surroundings. Taken together, the PCFs and density profiles complement each other to provide a complete statistical picture of the local structure of the nanocomposite. Inspection of the PCFs for the dry $Li^+$− and $Na^+$−montmorillonite systems show that these ions are coordinated by the PEO oxygen and, to a lesser extent, the silicate surface oxygen atoms (Figure 6). Coordination numbers are calculated by integrating the PCF to the "first minimum" and normalizing to the average density of the type of oxygen atom being considered. For consistency, the "first minima" were chosen by inspection as the point where the PCF curves appear to flatten out. Coordination numbers calculated in this way may not give ideal statistical values, but our intent is to show which species are dominant in coordinating the cations under different conditions. Coordination numbers calculated from the PCFs are given in Table 1. The PCF for $Na^+$ and the silicate surface oxygen also shows a sharp second peak and several smaller oscillations at larger distances. This is due to the periodicity of the silicate crystal structure, so that the second peak corresponds to the next nearest neighbor in the surface oxygen structure, and so forth. Because the PCF represents an average over many different configurations, accounting for many likely positions of the ion as it vibrates or diffuses, the peaks become rounded or smeared out. This "smearing out" becomes more evident with distance. At a large distance, even the PCF between an ion and the highly periodic silicate structure will converge to 1, when the PCF is normalized to the average bulk density of the silicate surface oxygen. A more mobile atom, which samples more possible positions, will also lead to more "smearing out" of these secondary or higher order peaks. The

**Table 1. Cation−Oxygen Coordination Based on Integration of Pair Correlation Functions[a]**

| species | number | PEO | surface O | total |
|---|---|---|---|---|
| $Na^+$ (dry system) | 24 | 5.1 (2.9 Å) | 1.2 (2.4 Å) | 6.3 |
| $Li^+$ (dry system) | 24 | 2.3 (3.5 Å) | 2.0 (2.7 Å) | 4.2 |
| species | number | $H_2O$ | surface O | total |
| $Li^+$ (surface) | 12 | 4.4 (3.0 Å) | 1.2 (2.6 Å) | 5.6 |
| $Li^+$ (gallery center) | 10 | 7.9 (3.0 Å) | 0.02 (2.6 Å) | 7.7 |
| $Li^+$ (overall) | 24 | 5.5 (3.0 Å) | 1.1 (2.6 Å) | 6.6 |

[a] Numbers in parentheses refer to the upper limit of integration of the PCFs in the calculation of these coordination numbers and correspond to the first minima of the PCFs. For the hydrated system, the number of overall $Li^+$ ions is greater than the sum of surface and gallery center ions because it includes ions that jumped between the surface and gallery center during the course of the simulation, and thus were not included in either the surface or the central Li.

**Table 2. Self-diffusion Coefficients of Li and Water in the Li−Montmorillonite/PEO Nanocomposite Based on 1-ns Molecular Dynamics Simulation**

| species | number | $D$ ($cm^2/s$) |
|---|---|---|
| $Li^+$ (surface) | 12 | $0.89 \times 10^{-8}$ |
| $Li^+$ (gallery center) | 10 | $2.0 \times 10^{-8}$ |
| $Li^+$ (overall) | 24 | $1.4 \times 10^{-8}$ |
| $H_2O$ | 133 | $8.0 \times 10^{-8}$ |

smaller size of the $Li^+$ ion makes it more mobile than $Na^+$, even within the cavity of the silicate surface. Because of this, the PCF between the $Li^+$ and the silicate surface oxygen is "smeared out" and begins to converge, even after the first peak.

The PCFs for the hydrated $Li^+$−montmorillonite system are shown in Figure 7. They show clearly that the $Li^+$ is primarily coordinated by the water oxygen atoms. Because PCFs show the PEO oxygen atoms to be clearly outside of the $Li^+$ coordination shell, they do not contribute to the calculation of the coordination numbers in the water-containing system. Table 1 shows the average number of oxygen atoms from the surface, PEO (for the dry system), and water (for the hydrated system) within the ions' primary coordination shells. All ions are considered together in each dry system. In the hydrated system, however, the ions in the gallery center are surrounded by water molecules, while oxygens from the silicate surface make up only a fraction of the coordination shell for the ions. In the absence of any external electric field, very few atoms move between a surface layer and the gallery center over the simulated time scale, so comparisons between surface ions and ions in the middle of the gallery are based on the ions that are clearly categorized as one type or the other throughout the simulation.

Table 2 shows the self-diffusion coefficients for water and $Li^+$ based on mean-squared displacement during the course of the 1-ns simulation. $Li^+$ cations in the middle of the gallery move faster than the cations near the silicate surface. This behavior reflects the ability of the surface to "trap" the $Li^+$ cations in the crystal lattice cavities or above negatively charged substitutional sites in the octahedral layer of the silicate. It should be noted, however, that the time scale of the simulation was not sufficient to statistically study the movement of ions from one surface cavity to another. The steric limitations of the rigid, stationary surface and the polarization of neighboring water molecules also impede the $Li^+$ mobil-

ity. At the surface, because there are relatively few water molecules in the hydration shell, the hydrating water molecules are more highly polarized and therefore more tightly attracted to the surface. Similarly, in studies of hydrated $Li^+$−montmorillonite, Sposito and co-workers have observed that surface complexes persisted while ions further from the surfaces formed a more mobile "diffuse layer" in two- and three-layer hydrates.[10]

When considering the mechanism of ionic motion, one may wonder whether the mobile ions drag their hydration shells with them or whether they move independently, exchanging one coordinating oxygen for another as they move. Water moves much faster than the $Li^+$ throughout the gallery. That water is moving so much faster than the $Li^+$ suggests that the local coordination environment of a $Li^+$ ion is rapidly changing as the coordinating water molecules move on, and new ones move into their place or as the water molecules fluctuate in their distance from the ion which they coordinate. This rapidly changing environment may facilitate the ion's motion because the ion may find itself momentarily lacking a coordinating oxygen and may easily move toward the vacated space, effectively taking advantage of the water dynamics.

To compare the rate of change of coordination environment to ion mobility, we looked at how often a $Li^+$ ion gained or lost a coordinating water molecule and compared ions near the surface to those in the center of the gallery. Molecules gained should equal molecules lost at equilibrium, and this is the case in our simulations. No attempt is made here to exclude molecules that leave and immediately return to the same hydration shell. In such a case, the ion would still have a chance to move into the free space while its neighbor was temporarily away. (In the case of conduction under an electric field, ions may be more likely to exchange neighbors because they, unlike water molecules, would migrate in a preferred direction.) For the gallery center, most ions exhibited over 300 losses or gains. More than $^2/_3$ of ions with fewer observed losses and gains—on the order of 50—belonged to the layers near the surface. On one hand, although surface ions may have statistically few water molecules, stationary surface atoms make up the remainder of their coordination shells, and therefore the surface ions have a less rapidly evolving coordination environment than ions in the middle of the gallery. On the other hand, the more mobile $Li^+$ cations in the middle of the gallery have a more rapidly evolving coordination environment.

## IV. Conclusions

Using computer simulations, we have shown that the intercalated polymer chains in a PEO-layered silicate nanocomposite are arranged in discrete subnanometer layers parallel to the crystalline silicate layers. Despite this ordering, the chains retain a disordered, liquid-like structure with no crystallinity or preferential ordering of the C−C−O bonds. This structure is in contrast to previously suggested configurations for intercalated PEO, but agrees well with more recent SANS experiments.

In the dry nanocomposites the cations reside primarily next to the silicate surface rather than being coordinated with PEO. In the hydrated nanocomposites, more than half of the cations present in the galleries exist in the layers near the silicate surfaces, partly inserted in the silicate surface cavities, and a few ions even appear to be translationally inhibited when burrowed within these crystalline cavities. Ions near the silicate surface move significantly more slowly than those in the center of the gallery. Water molecules, in general, diffuse more quickly than the ions.

Cations are primarily coordinated by water oxygen atoms, and to a lesser extent, by the silicate surface. In a hydrated system, the PEO oxygen atoms do not enter significantly into the cations' coordination cell. The ions' hydration environment changes most rapidly in the center of the gallery, where ion motion is faster. Because the changing coordination environment is related to the possibility the ions have for motion, the evolving hydration environment is related to the mobility of the ions.

**Acknowledgment.** This work was supported by the AFOSR. E.H. acknowledges an NSF Graduate Research Fellowship. We would like to acknowledge Dr. Juraj Bujdak for experimental data and useful discussions.

CM990676X